Construction and Building Materials 167 (2018) 757–767

Contents lists available at ScienceDirect

Construction and Building Materials

journal homepage: www.elsevier.com/locate/conbuildmat

Truss-type shear connector for composite steel-concrete beams

Luciano M. Bezerra [a,*], Wallison C.S. Barbosa [a], Jorge Bonilla [b], Otávio R.O. Cavalcante [c]

[a] Department of Civil and Environmental Engineering, University of Brasília, Brasília, Brazil
[b] Department of Mathematics, University of Ciego de Ávila, Ciego de Ávila, Cuba
[c] Federal University of Ceará, Department of Civil Engineering, Russas, Brazil

HIGHLIGHTS

- Experimental and numerical tests of new connector, the Truss Type shear connector.
- Truss-Type connector (TT-connector) cross section area is equivalent to 19 mm stud-bolt.
- In push out-out tests, TT-connector showed more resistance than the 19 mm stud bolt.
- The tests showed TT-connector has good ductility and stress distribution.
- TT-connector may be used when the equipment for stud-bolt application is unavailable.

ARTICLE INFO

Article history:
Received 27 October 2017
Received in revised form 26 January 2018
Accepted 30 January 2018

Keywords:
Composite structure
Steel-concrete beam
Shear connector

ABSTRACT

Shear connectors are important in composite steel-concrete beams. This work presents a new connector, named truss-type shear connector. This connector is an alternative to replace stud bolt in special situation. The connector's geometry was conceived aiming at low cost, easy execution, high resistance, and efficiency concerning slipping and uplift. Six specimens were constructed for push-out tests comparing this alternative connector with stud bolts. The behavior of the specimens was investigated for collapse, slipping and uplift. Experimental results were compared against numerical FE simulation showing good agreement and providing a global view of the truss-type shear connector behavior and its viability.

1. Introduction

The economic, technical, and scientific developments in the construction industry have brought about a great number of structural systems. Among them, steel-concrete composite structures have proved to be efficient from the structural and constructive points of view. As for the structural aspect, one can emphasize the better usage of materials' resistance properties, effectively exploring in a better way the potentials of concrete and steel [1]. The resulting combination of steel and concrete in composite beams, for example, provides lighter but more resistant structures. The use of composite structures with all its structural efficiency advantages [2] should be encouraged for bridge construction and even made more popular for medium and small construction too. As for the constructive aspect, steel-concrete beams can be built faster than reinforced concrete beams as the steel beam helps as support along the concrete slab curing process. Therefore, steel-concrete beams use less wood forms to cast the concrete slab. To accelerate even more the constructive process in making composite beams, precast concrete slabs can be associated with steel I-beam sections. Today, with increasing demand for infrastructures and dwelling, steel-concrete beam is a fast and cost effective system that may be well used for multi-story buildings and bridges.

The efficiency of steel-concrete beams, as resisting structure, depends highly to the interaction between two key structural elements: (a) steel I-beam and (b) overlaid concrete slab. Effective links between concrete slab and steel profile are required because these two materials have to act as a unique structure. Steel connectors are used as shear connectors, and, generally, they are welded to the steel profile flange and merged into the concrete slab – even though other options are available today [3].

One important characteristic for a shear connector in composite beams is its ductility. Shear connector may be classified in two categories depending of its ductility: rigid or flexible. Rigid connectors do not deform much under service load. They can provide good connection without showing much relative slipping displacement between steel I-beam and concrete slab. However, the collapse of rigid connectors is brittle. In this case, concrete failures for shear or crushing, and brittle failure takes place. Generally, such collapse

* Corresponding author.
E-mail address: lmbz@unb.br (L.M. Bezerra).

https://doi.org/10.1016/j.conbuildmat.2018.01.183
0950-0618/

is instantaneous showing no previous warning signals – which is not desirable for structural safety reasons. On the contrary, flexible connectors deform much more under load, allowing large relative slipping displacement between steel and concrete parts. This type of connector presents ductile collapse showing previous signs of breakdown. Flexible connectors are not quite good for some loading situations like oscillating loads. During an earthquake, shear connectors are subjected to reverse cyclic loading and flexible connectors deform more than rigid connectors, accordingly, they are more susceptible to early collapse. One example is the traditional headed stud bolt which is known to be a flexible connector and in this situation its strength is 17% lower [4]. Studs deform under service loads and have low performance under alternative loads, generally, breaking due to fatigue [4]. Rigid connectors, on the contrary, are not likely to go under early fatigue problem. For composite steel-concrete beams, the ideal shear connector should present very small slip displacement, rigid behavior, between steel and concrete when the composite beam is under service loads. However, the ideal shear connector should also present ductility at ultimate limit state. For an ideal shear connector, the characteristic of rigid connector is desirable for service load, and the characteristic of flexible connectors is sought in the ultimate limit state.

For the classification of shear connector as rigid or ductility, a criterion commonly accepted today is defined by the European Standard EN 1994-1-1: 2004 [5] for composite structures. The criterion is based on the characteristic slipping that each connector type may present, and this characteristic slipping can be measured in standard push-out tests.

The most commonly used shear connector today is the headed stud, or stud bolt [6,7]. This fact was mainly due to the productivity and the ease way such connector can be applied. The stud bolt is conceived to work as an arc welding electrode and it can be applied directly to the steel I-beam flange, or even over the metal sheeting of the steel decking over the steel I-beam flange. As a result of the high degree of automation and practicability in the construction site, the stud bolt is the connector commonly used all over the world. One disadvantage in the use of stud bolt is when the composite structure is submitted to fatigue. Besides, for the application of this type of connector, specific welding equipment and high electric power, approximately 225 kVA generators, at the construction site are needed. These requirements limit the application of stud bolt connectors [3]. Moreover, there are also some problems involving the performance of stud connectors and their installation [8]. One problem is the reliability of the installation automation of the welding process. Another problem is the relatively small load that each stud bolt can withstand. Therefore, in steel-concrete composite beam, a large number of studs have to be applied. There are several other parameters that influence stud connectors like the shank diameter, the height of the stud, the bedding height, among others [9,10].

In the context of some countries, the installation of studs carries additional concerns, like the difficult to get the special welding machine and enough electric power in remote construction site. The appropriate welding machines have high cost and difficult acquisition for small construction companies operating in isolated areas away from large urban centers. Depending on the location of the construction site, the need for extra energy generator and a good energy infrastructure can make steel-concrete composite structures more expensive, if stud bolts are used. Therefore, the choice of the connector type, their correct size, and their execution are of great importance – since they determine the good or bad interaction degree, and the ways stresses are distributed, between the two materials, i.e. steel and concrete.

There are many recent researches on new types of shear connectors that could substitute the traditional stud bolt [11]. There are alternative shear connectors applied with welds, bolts and nuts, and even connectors that may be assembled and disassembled (i.e. mountable and demountable connectors). Recently, alternative connectors have deserved more attention in the technical literature with many motivations and a wide variety of ideas and gadgets presented [11–14].

This research shows a new type of alternative connector, the Truss-Type (TT) Shear connectors made of common steel type CA-50 bars – commonly used in reinforced concrete structures. The geometry of the alternative TT connector was conceived targeting: (a) no need for special equipment for the installation of the connector, (b) low cost of production, (c) easy installation and execution, (d) high resistant value, (e) efficiency concerning relative slip and uplift resistances between steel section profile and concrete slab. The approach of numerical and experimental studies is of great value to understand the behavior of the proposed alternative TT connector. This approach is considered in this research.

2. Conception of the truss-type connector

The shear connectors designed for this research were built using steel rebar type CA-50 for reinforced concrete structures and bent in triangular shape with geometry as illustrated in Fig. 1. In that figure, for bending downwards, the concrete slab and the steel I-beam flange act, respectively, as the top and bottom chords of a truss, and the legs of the TT connector are like truss diagonal elements. These observations are important to explain the name given to this connector: Truss-Type (TT) shear connector. The goal in developing TT shear connector is also to get an alternative connector that could be used in situations where the use of stud bolts is not possible. The TT shear connector here presented has been registered in the Brazilian National Institute of Industrial Property under the number: BR302016002949-0. Alternative connectors must be well studied in order to become reliable for engineering practice. Studs are already well acknowledged by many Standards, including the European Code EN 1994-1:2004 [5] and the AISC Code [15], among others, but new options of shear connectors are always welcome. Therefore, for the experimental comparison between TT connectors, 19 mm (3/4") diameter and, approximately, 130 mm (5 3/16") height stud bolts were used.

For the assembly of the TT connector, CA-50 bar with 1/2" (12.5 mm) diameter which is very mush used in civil construction was chosen. The reason for 12.5 mm diameter is to approximate the cross section area of the two legs of the TT connector to the cross section area of the 19 mm stud bolt. The two legs of the TT connectors substitute one stud bolt with 19 mm. Comparing the steel cross section area of the Stud Bolt with 19 mm diameter (SB-19.0) and TT connector with 12.5 mm diameter (TT-12.5), it can be seen that the cross section area of the SB-19.0 is $A_{SB} = 2.84\ cm^2$ and the cross section area of the two legs of the TT-12.5 (see Fig. 1) is $A_{TT} = 2 \times 1.27 \approx 2.53\ cm^2$. Therefore, both connectors are about the same, even though $A_{SB}/A_{TT} \approx 1.12$, or A_{SB} has 12% more cross section area than the two legs of the TT connector.

With respect to the mechanical properties, CA-50 steel bar for TT-12.5 has yielding stress of 595.3 MPa and ultimate stress of 716.6 MPa, while SB-19.0 presents a yielding stress of 345 MPa and ultimate stress of 415 MPa. TT-12.5 mm and SB-19 mm connectors are about the same height, respectively, with 130 mm (see Fig. 1). For the TT connector, a piece of 40 mm in length was welded to the top angle (see Fig. 1) of each connector to resist the uplift. Such piece plays an analogous role as the stud-bolt head. The link between the truss connector and the steel profile was made with butt welds applied on both end sides of the TT connector legs welded to the steel I-beam flange (see Fig. 1). Shielded Metal Arc Welding (SMAW) was applied with E70 electrodes. Each of the four weld strings (at each side of the TT connector legs) was executed with 35 mm of length (see Fig. 1). For the push-out tests

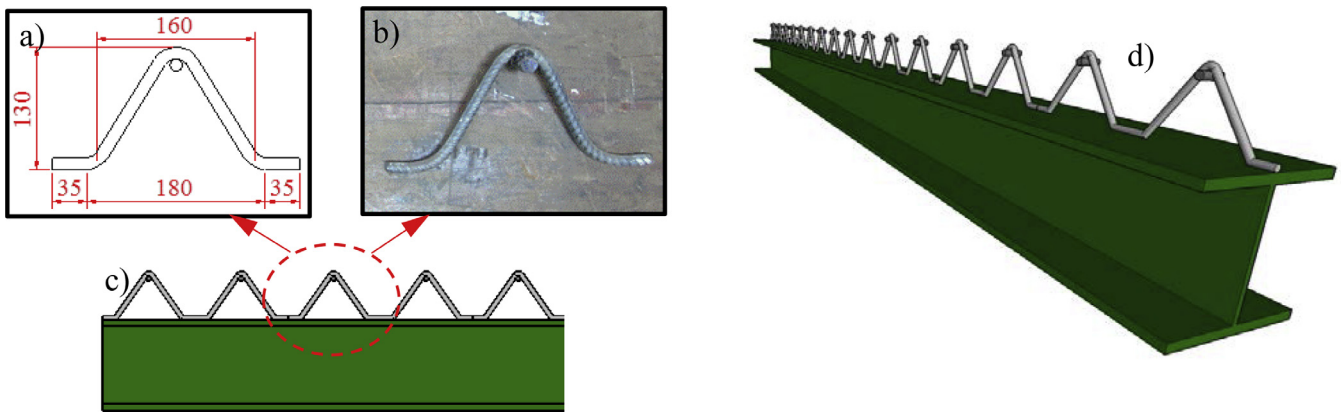

Fig. 1. TT connector details: (a) Measures, (b) Triangle unit, (c) Frontal view, (d) Perspective view.

eight TT connectors, for each experimental specimen, was prepared and fixed independently from the others. However, a longer series of TT connector can be industrially produced – as suggested in Fig. 1d.

3. Experimental program

To analyze the behavior of the TT connector developed in this work, experimental push-out tests are carried out in accordance with the provisions of the European Code EN 1994-1:2004 [5]. The tests were held at the University of Brasilia. During the push-out tests, the applied load, the relative slip displacement, and the detachment or uplift displacement between the steel I-beam flange and the concrete slabs were monitored.

3.1. Push-out tests

The experimental evaluation of the resistance capacities of both types of connectors consists of push-out tests of SB-19.0 and TT-12.5 specimens. Six experimental specimens: three with SB-19.0 connectors and three with TT-12.5 connectors, are accomplished. Standard specimens were constructed with A36 steel I-section beam and two reinforced concrete slabs with concrete which medium strength is f'_{cm} = 34 MPa. Steel I-section beams of the W250x73 profile were employed to all the six specimens to test. They are equivalent to HEB 260, European profile, recommended by Standard EN 1994-1-1:2004 [5]. Table 1 presents the nomenclature and details of the specimens analyzed in this work. In each specimen, eight shear connectors were welded, four at each flange of the steel I-section for both SB-19.0 and TT-12.5. The behavior of the TT connector compared to the SB behavior is done by the correlation between applied loads and relative slip and uplift displacements to the specimens. Slip and uplift displacements takes places between the steel profile and the concrete slab surfaces.

The six specimens described in the last column of Table 1 have standard concrete slabs reinforced with CA 50 steel bars of 10.0 mm. Fig. 2 shows the details of the reinforcement bars of the concrete slabs for the experiments of the proposed TT-12.5 shear connector, the same concrete slab reinforcement was used for the SB-19.0 connector specimens. It is noted that 10 cm were added to the height of each model slab, so that they could withstand connectors with different extension; and another layer of horizontal reinforcement steel was added to the slabs to keep the reinforcement steel rate – Fig. 2 shows more details.

Table 1
Characteristics of the models for the push-out tests.

Shear Connectors		Nomenclature with diameter	Specimen Nomenclature
Type	Diameter (ϕ)		
Stud Bolt	19.0 mm	SB-19.0	SB#1, SB#2, SB#3
Truss-Type	12.5 mm	TT-12.5	TT#1, TT#2, TT#3

The vertical displacement of the slabs in relation to the I-section steel profile and the horizontal displacements between the slabs were monitored through LVDTs (Linear Variable Differential Transducer). The LVDTs were positioned as shown in Fig. 3. Two LVDTs H1 / H2 were used to check for the horizontal separation between slabs or the uplift displacements. Two LVDTs V1 / V2 monitored the vertical or slipping displacement of the steel profiles with respect to the concrete slabs. The LVDTs were fixed with mechanical clamp devices and magnetic bases, as indicated in Fig. 3. The tips of the vertical LVDTs were in contact with metal plates bonded in the I-beam; the tips of the horizontal LVDTs were directly in contact to the concrete surface of the slabs, and positioned perpendicularly to the specimen vertical axis. The horizontal LVDTs were placed at the height of the connectors vertices, located at 250 mm distance from the ends of the concrete slabs. The vertical LVDTs were placed at a 325 mm distance in relation to the upper end of the concrete slabs of each specimen. In Fig. 3, details of the positioning of the LVDTs during the experimental tests are presented. The load was applied to the steel I-beam and transmitted to the concrete slabs through the shear connectors. The values of the loads applied to the specimens were controlled by a load cell placed in line and above the hydraulic actuator as illustrated in Fig. 3. The applied loads were registered along the load steps and later correlated to the vertical slip and horizontal uplift displacements for each specimen tested.

The specimens were assembled for the tests in the Civil Engineering Structural Laboratory at University of Brasília. In the lab, among the frames, the one available for the tests was a fixed frame made of steel with carrying load capacity of 2000kN. The frame was at the same time employed to test other structural prototypes and could accommodate specimens up to 355 cm high. Specifically, for the push-out tests of the SB-19.0 and TT-12.5, after preparation, the specimens resulted 80 cm high. To enable the application of load, the specimens had to be lifted to be closer to the load cell. With the help of the lab crane, strong concrete blocks available in the lab were stacked. The blocks were placed over thin layers of plaster to create very regular contact surfaces [16]. A steel plate was also placed on top of the last block, and the lab crane placed the SB-19.0 and TT-12.5 specimens on the top of the concrete

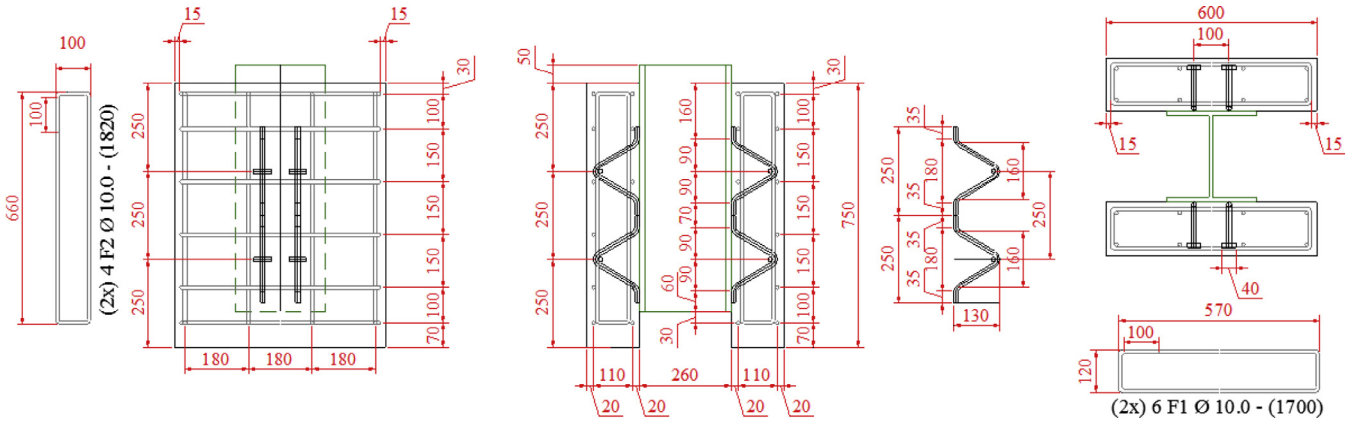

Fig. 2. Concrete slab reinforcement bars for the TT-12.5 push-out tests – dimensions in mm.

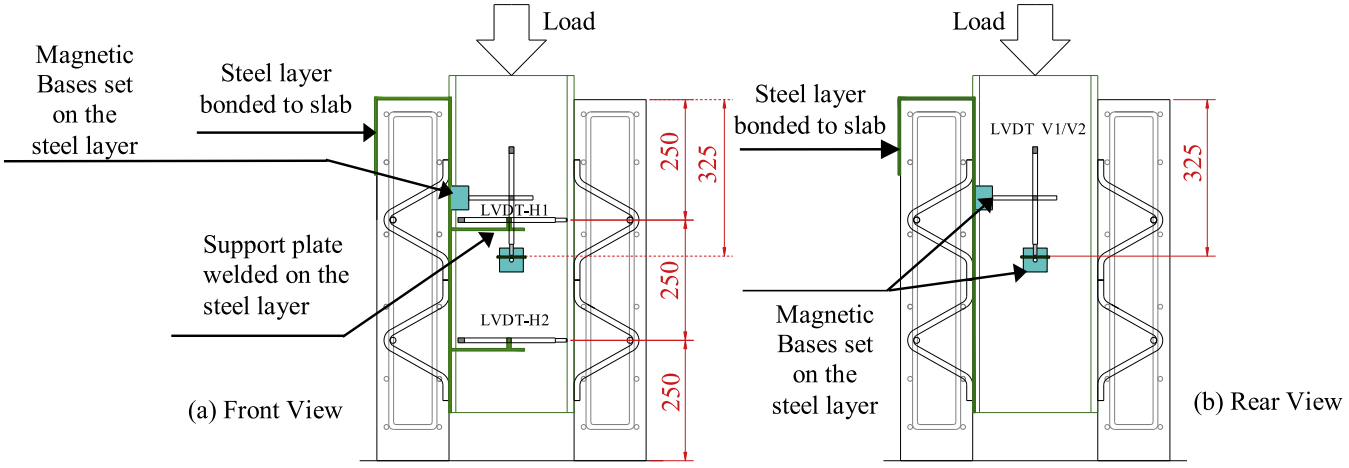

Fig. 3. Positioning of LVDTs to measure up-lift and slip displacements.

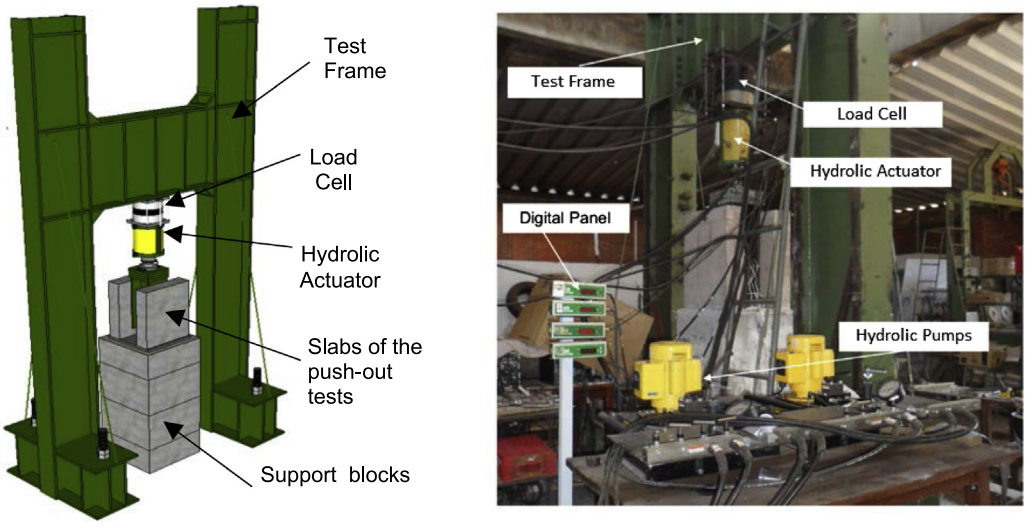

(a) Testing Frame - Perspective view (b) Positioning of specimens for push-out tests

Fig. 4. Testing system used for push-out tests.

blocks. For safety, the push-out specimens were protected with steel chains to prevent the fall of large pieces of debris at rupture of the specimens. A detailed scheme and photo of the resulting push-out testing assemblage are presented in Fig. 4a and b.

3.2. Data acquisition system

The displacement values obtained from the LVDTs were registered for each load step with the aid of the Spyder-8 data

acquisition modules. The manufacturer of these modules is the German company HBM (Hottinger Baldwin Messtechnik GmbH). The data acquisition software used was Catman, version 4.5. The data from Spyder-8 modules was stored in a notebook. One of these modules was used for the LVDTs used in each test. The load data acquisition was made by directly reading the values on a digital panel. The load values at rupture and immediately after it were registered through film recordings performed along all the push-out tests. The display showed the load values at the load cell to which it was connected to. The load cell was placed between the hydraulic actuator and the frame horizontal-beam. Fig. 4a and b illustrate this assemblage.

The load was applied by the electric hydraulic pump shown in Fig. 4b placed in line with the load cell. That pump allowed the force control which value can be seen on the digital panel display. The estimated rupture load is 800 kN. Loading recommendations, as required by European Standard EN 1994-1-1:2004 [5], were followed, i.e. application of pre-loads in 25 cycles ranging from 5% to 40% of the estimated ultimate load, respectively, 40 kN–320 kN. After these 25 cycles, the specimen under test is subjected to increasing load up to collapse in no less than 15 min. When achieving the maximum testing load, the load is reduced in 20% to allow the ductility classification of the tested connector.

4. Experimental results and discussions

The push-out tests were conducted considering the procedures described in reference [5], which is accepted as an international standard for evaluating new shear connectors for composite beams. The push-out tests of the six specimens (see Table 1) allowed the evaluation of the rupture load, the relative vertical and horizontal displacements between the concrete slabs and the I-beam profile, the final shape of the connector and the crack distribution on the outer surface of the concrete slabs. The SB-19.0 and TT-12.5 specimens were compared in terms of displacements and collapse loads. Fig. 5 presents the curves of slip vs applied load of all the six specimens tested. The average reading of the slipping displacements were done from the two LVDTs V1 and V2 on each specimen during the tests. P_{max} is the maximum load value reached for each tested specimen. The main results from the push-out tests of the six specimens are reported in Table 2. The tests were considered valid, as the three maximum load (P_{max}) obtained did not differ in more than 10% of the average rupture loads – considering the specimen series with identical configuration (i.e. SB-19.0 and TT-12.5 series). Note that the rupture loads obtained in the six tests were above the estimated value of 800 kN for the tested connectors.

Standard EN 1994-1-1:2004 [5] suggests Eq. (1) to calculate the design resistance of the shear connectors evaluated by push-out tests.

In Eq. (1), f_u is the minimum resistance to rupture of the connector's material; f_{ut} is the real resistance to rupture of the connector's material; P_{Rk} is the lowest rupture load value of tested models (divided by the number of connectors) reduced in 10%; and γ_v equal to 1.25 is the partial safety coefficient, recommended by EN 1994-1-1:2004 [5]. The design resistant load obtained by equation 1 is for one shear connector; therefore, by using equation 1, the design resistant load values obtained for SB-19.0 connectors is 58.71 kN and 104.5 kN for TT-12.5 connectors. Each push-out test was executed with eight connectors, thus the design resistance for SB-19.0 is 469.7 kN and for TT-12.5 is 836.0 kN. As a result, TT-12.5 connectors are more resistant than SB-19.0 connectors.

$$P_{Rd} = (f_u/f_{ut}) \cdot (P_{Rk}/\gamma_v) \quad (1)$$

4.1. Vertical slipping

The relative vertical slip between the steel I-beam and the concrete slabs of SB-19.0 and TT-12.5 were observed during the experimental push-out tests through LVDT-V1 and LVDT-V2 (see Fig. 3) placed symmetrically in relation to the steel I-beam web of each specimen. The results obtained are the slipping curves as function of the applied loads in Fig. 5. The average vertical slipping values registered by LVDTs-V1 and LVDTs-V2 are presented in Fig. 6a. With the data on the slipping displacement, the procedure to classify the connectors concerning their ductility was carried out. In Fig. 5, it was possible to apply the reduction of 20% to the loads reaching the maximum values.

Moreover, in Fig. 5, the characteristic resistant load P_{Rk}, which is 10% lower than the maximum load, can also be found together with its respective vertical slip displacement (δ_u) on the graphs. The characteristic slip δ_{uk} is defined as 90% of δ_u. According to EN 1994-1-1:2004 [5], connectors that lead to characteristic slipping values, δ_{uk}, higher than 6.0 mm are classified as flexible connectors and if δ_{uk} values are lower than 6.0 mm, connectors are classified as rigid. Observing all the graphs in Fig. 5, it is noticed that SB-19.0 and TT-12.5 series showed values of δ_{uk} higher than 6.0 mm.

Therefore, both can be classified as flexible connectors. According to EN 1994-1-1:2004 [5], flexible connectors show plastic behavior, with good stress distribution between the connectors for service loads. Fig. 5 shows the values of δ_u obtained for 90% of rupture load and Table 3 shows the calculated values for δ_{uk} and the classification of the connectors tested regarding their ductility – following EN 1994-1-1:2004 [5] criteria.

4.2. Horizontal displacement – Uplift

In composite beams, besides longitudinal shear forces, connectors are also subjected to forces that are transversal to the steel I-beam longitudinal axis. These forces cause vertical separation between the concrete slab and the I-beam (effect known as uplift). In general, the transversal forces that appear are much lower than the longitudinal shear forces, and in practice, it is not necessary to calculate them [1]. To monitor the horizontal displacement of the slabs (uplift), LVDTs (H1 and H2) were used. Their bases were fixed on one lateral concrete slab and the other extremes touched the other slab (see Fig. 3). Those LVDTs were mounted at two different heights corresponding to two different centroid rows of connectors. To save space in this paper, only the average uplift results (for LVDTs H1 and H2) of each specimen tested is shown in Fig. 6b. In TT-12.5 specimens, there were higher uplift values on the inferior part of the slabs for load values close to P_{max} (maximum test load) and during the stage of load decrease by the end of the push-out tests. In Fig. 6b, one can observe that the TT-12.5 connectors led to greater maximum loads and also greater uplift values. In Table 4, the experimental uplift results obtained from the six tests are presented. In that table, P_{max} is the maximum load held by the specimen; Up_{80} is uplift for $0.80P_{max}$, and δ_{80} is the slipping for $0.80.P_{max}$. The connector's resistance to uplift is verified in the following way: the transversal separation between the steel I-beam section and the concrete slabs, measured when the connectors are subjected to 80% of their ultimate load, must be inferior to 50% of the corresponding longitudinal slipping. Otherwise, the connection capacity is not satisfactory [5].

From Table 4, both connectors fulfill the ratio recommendation (U_{p80}/δ_{80}) suggested by [5]. In the same table, for the TT-12.5, Up_{80} average was 0.93 mm, while for the stud bolts; the average of Up_{80} was 0.84 mm. These uplift average values are close. The resistances to uplift, measure with the Up_{80} values, are resistances relative to the 80% of the maximum load reached in each specimen. According to the criteria of EN 1994-1-1:2004 [5], SB-19.0 presents a better

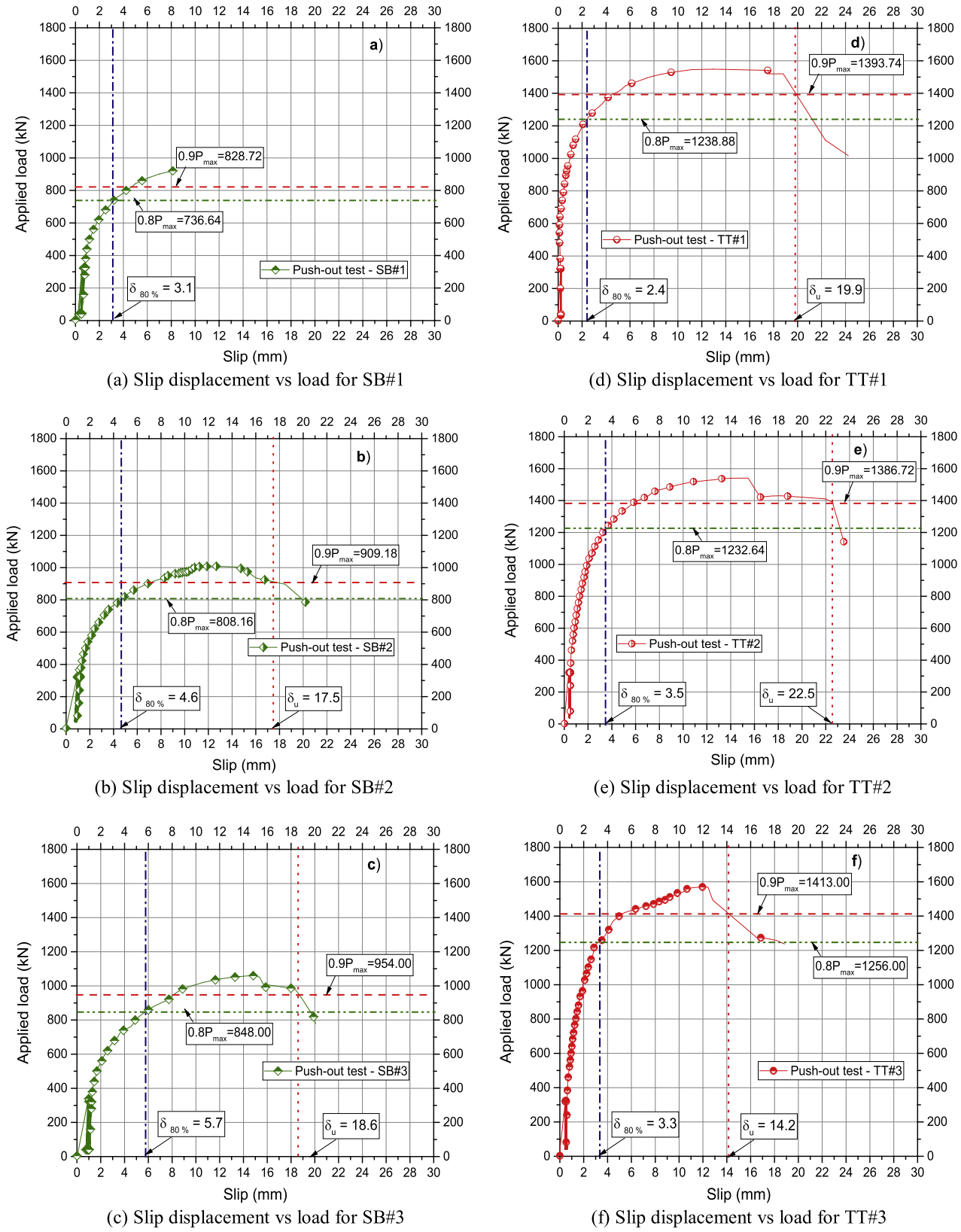

(a) Slip displacement vs load for SB#1

(d) Slip displacement vs load for TT#1

(b) Slip displacement vs load for SB#2

(e) Slip displacement vs load for TT#2

(c) Slip displacement vs load for SB#3

(f) Slip displacement vs load for TT#3

Fig. 5. Slip vs load average curves from LVDTs V1 and V2 and characterization of connector flexibility.

resistance to uplift. The ratio $0.93/0.84 \approx 1.11$ shows 11% more uplift for TT-12.5 compared to SB-19.0 – noting that TT-12.5 reached a much higher maximum load than SB-19.0. The mechanical properties of TT-12.5 are higher than SB-19.0; the values (yield stress, ultimate strength) in MPa are: (595.3, 716.6) for TT-12.5 and (419.5, 585.8) for SB-19.0. Despite better properties for TT-12.5, the better resistance to uplift for SB-19.0 could be related to various factors [17,18], among them, shape, cross

Table 2
Rupture loads for all tested models.

Connector Types	Specimen Number	P_{max} Total (kN)	Average P_{med} Total (kN)	P_{cmax} per Connector (kN)	Average P_{cmed} per Connector (kN)	Lowest Design Resistance according to Eq. (1)* [5] P_{Rd} (kN)
SB-19.0	SB#1	920.80	997.00	115.10	124.63	58.71
	SB#2	1010.20		126.28		
	SB#3	1060.00		132.50		
TT-12.5	TT#1	1548.60	1555.13	193.58	194.14	104.50
	TT#2	1540.80		192.60		
	TT#3	1570.00		196.25		

* In Eq. (1) in MPa: (a) for SB-19.0, $f_u = 415$, $f_{ut} = 585.8$, and (b) for TT-12.5, $f_u = 540$, $f_{ut} = 716.6$.

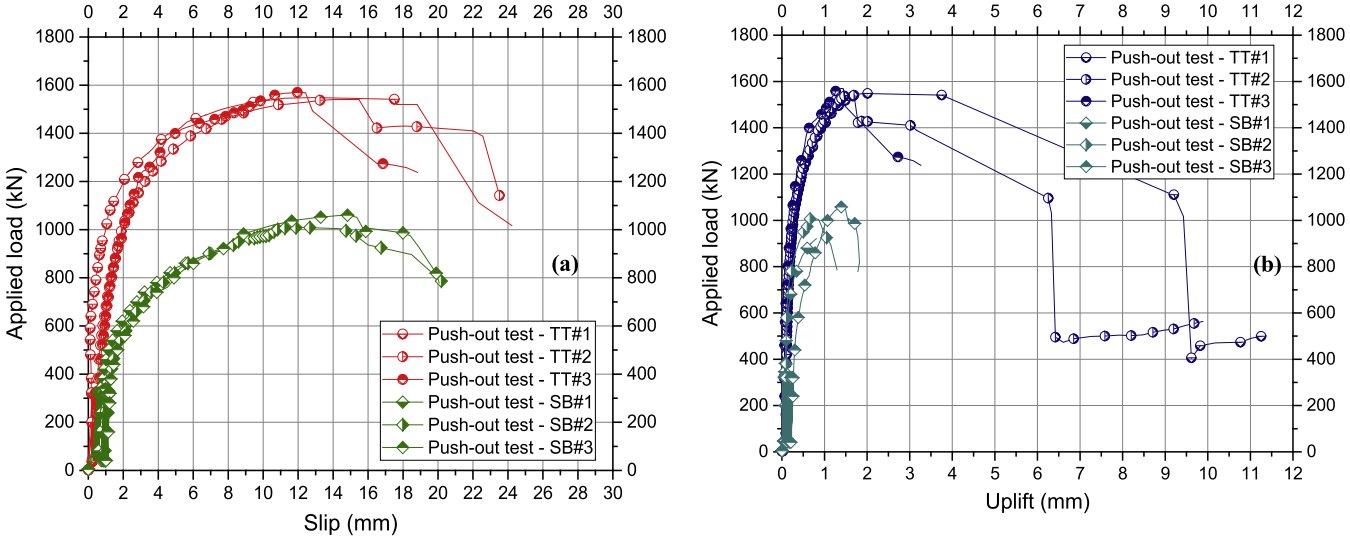

Fig. 6. Average curves: (a) slip vs load (LVDTs V1 and V2), (b) uplift vs load (LVDTs H1 and H2).

Table 3
Classification of the connectors according to their ductility.

Connector Type	Specimen Number	δ_u (mm)	δ_{uk} (mm)	Classification According to EN 1994-1-1:2004 [5]	Type of Collapse
SB-19.0	SB#1	N.A	N.A.	N.A.	Weld break between stud bolt and beam flange.
	SB#2	17.50	15.75	Flexible	
	SB#3	18.60	16.74	Flexible	
TT-12.5	TT#1	19.90	17.91	Flexible	CA-50 steel bar break close to weld, concrete failure too.
	TT#2	22.50	20.25	Flexible	
	TT#3	14.20	12.78	Flexible	

Table 4
Registered uplift for all tested models.

Tests	P_{max} (kN) per test	P_{max} (kN) average	Up_{80} (mm)	Up_{80} Average (mm)	Up_{80}/δ_{80} (%)
SB#1	920.80	997.00	0.52	0.84	17%
SB#2	1010.20		0.49		11%
SB#3	1060.00		1.50		26%
TT#1	1548.60	1553.13	1.10	0.93	46%
TT#2	1540.80		0.90		26%
TT#3	1570.00		0.80		24%

section area, and anchorage of connectors. The cross section area ratio between SB-19.0 and TT-12.5 connectors (A_{SB}/A_{TT}) is 1.12 or 12% more for SB-19.0.

5. Numerical modeling of the push-out test

It is noted that experimental methods are often unable to give the complete state of displacement, strain and stress through the use of single experimental techniques like push-out tests. In contrast, the modern finite element method, among other numerical methods, can yield a much more precise picture of the complete state of stress, strain and displacement in a body under load. Therefore, as a complement to the experimental push-out tests and for a better understanding of the behavior of the TT connector, the numerical modeling of the push-out test using FE analysis in ABAQUS [19] software was developed in this research.

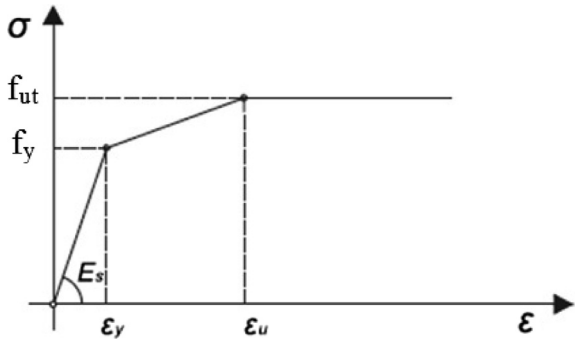

Fig. 7. Stress-strain relationship for steel material.

Table 5
Steel properties.

	TT-12.5	Rebars	Beam
E_s (MPa)	195300	194500	200000
f_y (MPa)	595.3	591.6	250
f_{ut} (MPa)	716.6	722.4	400
ε_u (%)	0.6	0.6	1.0

The three-dimensional geometry of the push-out test specimen, the non-linearity of steel and concrete were considered in the numerical model. In order to obtain accurate results from the FE analysis, all components in touch with the shear connection are properly modeled which means that in the specimen, the main components affecting the behavior of shear connection are considered: concrete slab, reinforced bars inside the concrete slab, truss-type shear connectors, steel I-beam, and contact interaction with large slip displacement. The post-failure behavior is also considered and in this stage, the numerical convergence during the push-test analysis is difficult to be accomplished. For that reason and based on the research by Qureshi and Lam [20], the simulation of the push-out test has been done in ABAQUS/Explicit dynamic procedure [19,21]. Therefore, a quasi-static simulation, using explicit dynamic procedure, with slowly load application is put into practice to minimize the inertia effects. For more details on this procedure see Qureshi and Lam [20].

5.1. Modeling of steel

Based on different researches on modeling of concrete-steel composite structures, a von Mises' criterion was adopted for steel [20,22,23]. For this purpose the option (*PLASTIC) available in ABAQUS [19] was utilized. ABAQUS uses the classic rule of associated plastic flow and the isotropic yielding [19,21] to represent the behavior of steel material in the three-dimensional (3D) space of stresses. Based on the numerical studies [23] to simulate the 3D behavior of the steel material accurately, ABAQUS [19,21] just needs the steel's uniaxial stress-strain curve which is represented, in this research, by the stress-strain curve as shown in Fig. 7. In this curve, the TT-12.5 material behavior is initially elastic with Young's modulus (E_s) followed by a strain hardening and then yielding. The steel properties of the TT-12.5 connectors and the reinforcing bars inside the concrete slab are specified in Table 5. For the I-section beam, the properties of ASTM A-36 steel (Section 2 in this paper) were used, as specified in Table 5. The density of all steel components was assumed to be 7800 kg/m^3.

5.2. Modeling of concrete

In this work, concrete material was modeled considering the Concrete Damaged Plasticity (CDP) model available in ABAQUS [19,21] based on the researches by Lubliner et al. [24] and Lee and Fenves [25]. The CDP model is acknowledged to provide a general ability to model efficiently the behavior of concrete and other quasi-brittle materials. The above mentioned model for concrete [24,25] has been previously used exhibiting very good results [20,22,23]. The CDP model follows non-associated plasticity flow rule, whereby the plastic potential function and the yield surface do not coincide with each other. For the flow potential ABAQUS [21] uses the Drucker-Prager hyperbolic function. For calibration, different parameters must be defined in CDP model. The concrete properties for the CDP model are: (a) Initial modulus of elasticity, E_o = 26 GPa, (b) Poisson's ratio ν = 0.2, (c) concrete weight density γ_c = 2500 kg/m^3, and (d) an angle of dilation of 13°. E_o and γ_c were taken based on average values from experiments in the Civil Engineering Laboratory at University of Brasilia, and ν = 0.2 was assumed. The value for the angle of dilation was taken from [26–28]. For the other plasticity parameters, the default value suggested by ABAQUS has been assumed [19]. With such data, ABAQUS is able to represent concrete damage according to CDP model, for more details see reference [29]. In relation to the concrete compression behavior, given the uniaxial stress-strain curve, ABAQUS [19,21] can establish the multiaxial stress state behavior. Based on different researches [20,23], in this study, the uniaxial stress-strain curve for concrete given by EC-2 [30] was used. The concrete tensile behavior has been defined taking into account the recommendations of Qureshi and Lam [20].

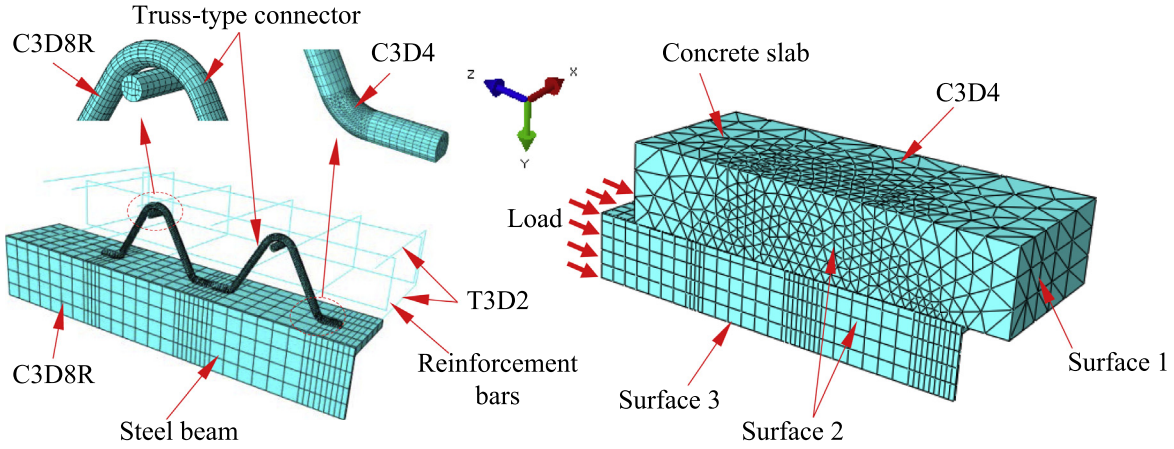

Fig. 8. Finite element model.

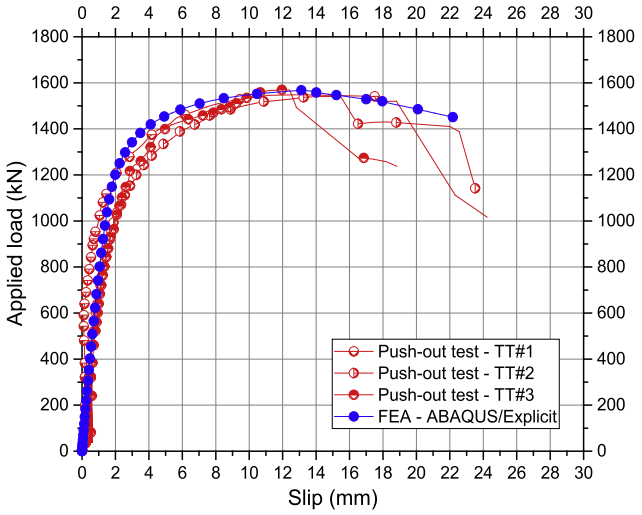

Fig. 9. Load applied versus slip for push-out specimens (TT-12.5).

The analysis is carried out using ABAQUS/Explicit dynamic analysis program, but in this investigation static solution is required; therefore, the top of the steel beam in the push-out test arrangement was very slowly loaded by applying a constant velocity of 0.25 mm/s.

5.3. Finite element type, mesh and boundary conditions

Combinations of strut elements and solid elements, which are available in the ABAQUS [19] explicit element library, are used to model the push-out test specimen. Therefore, two-node elements (T3D2) are used to model the reinforcement bars. Combinations of eight-node elements (C3D8R) and four-node elements (C3D4) are used to model the TT shear connectors. Four-node elements (C3D4) and eight-node elements (C3D8R) are used to model the concrete slab and steel beam respectively. The mesh in the concrete slab is employed with variable finite element density, refining the mesh towards the slab to TT-12.5 interactive contact area. In the TT-12.5 connector the mesh has a uniform size (see Fig. 8).

All nodes along surface 1 are restricted from moving in the Z direction (see Fig. 8) – see the axis directions in Fig. 8 too. All steel beam flange nodes, concrete nodes and steel wire mesh nodes, which lie on the other symmetry surface (Surface 2) are restrained in the X direction. In the steel beam at mid depth (Surface 3) all nodes are restrained from moving along the axis of symmetry, i.e. in the Y direction. The contact between the concrete slab and the steel I-beam surfaces was defined as frictionless and rigid. Based on numerical modeling research on the behavior of stud bolt shear connector in push-out test [20,22,31], in this study, the contact between TT connectors and concrete has been considered as rigid too.

5.4. Numerical results

The experimental load-slip curves obtained for TT-12.5 specimens are compared with the numerical curve obtained from the FE analysis, as shown in Fig. 9. Good agreement has been achieved between experimental and numerical load-slip curves. It can be seen that the FE models successfully predicted the resistance and the load-slip behavior of TT-12.5 shear connectors. In Fig. 10, it is noted that TT-12.5 legs work primarily under tension (T) and compression (C). It can also be observed that the higher stresses in the TT connector are concentrated at the base. Fig. 11 shows that the higher stresses in concrete are concentrated, mainly, in the front part of the legs of the TT connector, near its base. From the observation of the numerical model behavior near the failure, it can be established that this occurs due to the combined effects of concrete crushing near the connector and shearing, bending and tensioning at the base of the connector. This numerical result is in perfect agreement with the experimental results of the TT shear connector at failure, as can be seen in Fig. 12.

At the final stages of the push-out tests, due to the higher slip values, greater deformations were observed for the TT connectors and also in the concrete slabs of the specimens. The quality of the numerical simulation, can be detected when Figs. 10 and 11 are compared with the experimental results shown in Fig. 12(a), (b) and (c). Such figure was obtained from some TT-12.5 specimens that were cleaned up after the test (Fig. 12(a) and (b)). One specimen was cut with a cutting blade for reinforced concrete as shown

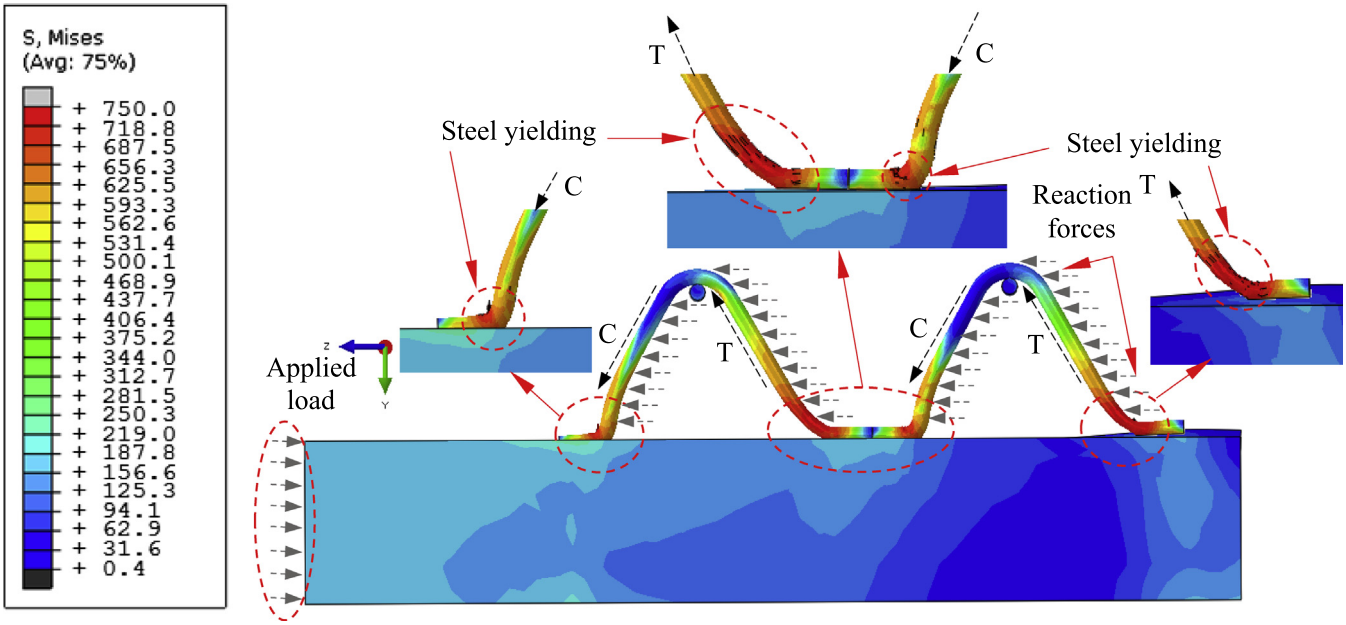

Fig. 10. Stress contours (in MPa) and TT deformed shape at failure in push-out tests of TT-12.5.

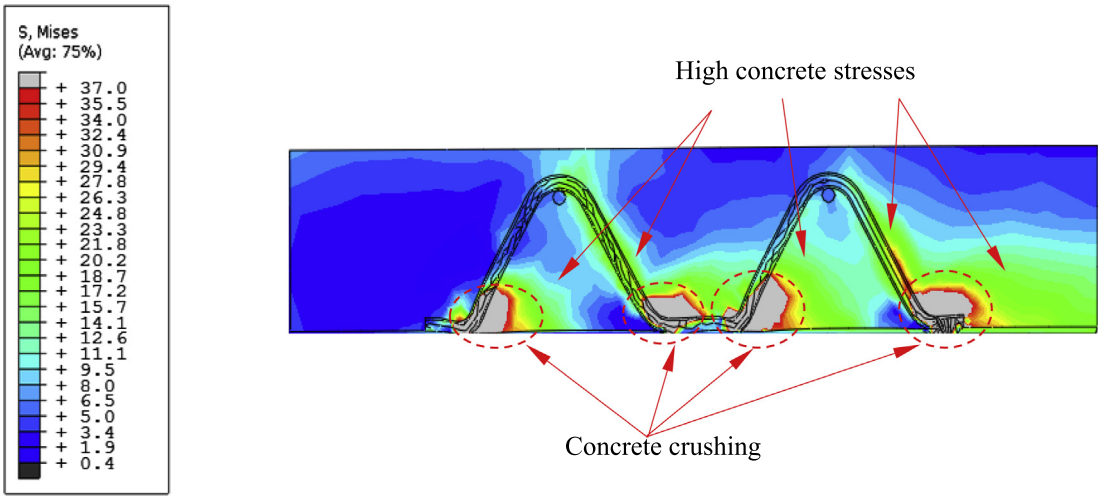

Fig. 11. Stress contours (in MPa) and concrete failure in push-out specimen TT-12.5.

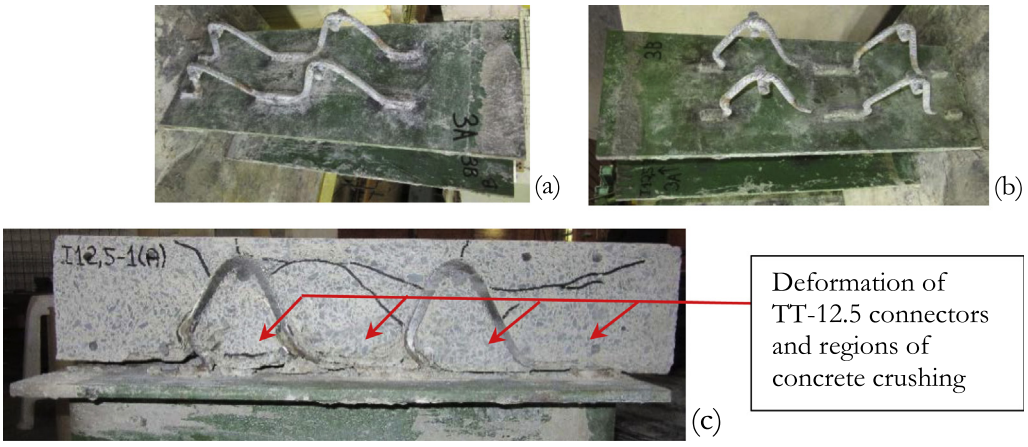

Fig. 12. Failure in push-out of specimens of TT-12.5.

in Fig. 12(c). The cut of the specimen was carried out longitudinally in a row of TT connectors. The crushing of the concrete material in the vicinity of the sliding interface between the steel I-beam profile and the concrete slab can be observed as indicated in Fig. 12(c).

6. Conclusions

In this paper a new and efficient alternative connector named Truss Type shear connector, or TT-12.5 for steel-concrete composite beams was presented. TT-12.5 was conceived from 1/2" (12.5 mm) steel bars and its cross section areas is 12% less than the Stud Bolt connectors with 19.0 mm diameter (SB-19.0). Experimental push-out tests of TT-12.5 and SB-19.0 connectors were conducted. Such tests registered the load vs. slip and load vs. uplift of each specimen showing the load capacity and ductility of each connector tested. The tests followed the provisions given on the European Standard EN 1994-1-1:2004 [5]. From the push-out tests, the following observations were taken: The ultimate resistance for TT-12.5 specimens is 1553.14 kN on average (or 194.14 kN per conector), against an average of 997,0 kN for SB-19.0 (or 124,63 kN per conector). The calculation of design resistance for each shear connector (P_{Rd}), according to European Standard EN 1994-1-1:2004 [5], led to P_{Rd} = 62.45 kN per SB-19.0 and P_{Rd} = 104.50 kN per TT-12.5. The push-out tests allowed the classification of both types of connectors as flexible. TT-12.5 shows good plastic deformation behavior at rupture. There is also a better stress distribution for TT-12.5 connectors as there are two cross section legs compared to one cross section for SB-19.0. Given the results obtained from Up_{80}/δ_{80} ratio, SB-19.0 and TT-12.5 meet the criteria of European Standard EN 1994-1-1:2004 [5], with Up_{80}/δ_{80} ratio $\leq$50%. The TT-12.5 connector presented rupture by tension at the end of one of its leg. The weld length adopted at the end of the TT-12.5 legs was enough to resist the applied loads. Welding can be performed with usual electrodes and welding machines, without the need of specific equipment as required for SB-19.0 connector usage. TT-12.5 connectors can be supplied already folded in the triangular shape and ready for direct application on the steel I-beam flange of a composite steel-concrete structure. The TT-12.5 connector developed in this research may be an alternative for use in composite steel-concrete beams. The material to manufacture TT-12.5 connector can be easily found and its manufacturing and installation are simple. TT-12.5 connector can be used when stud bolts installation is not possible, economically feasible, or when the appropriate equipment for SB-19.0 application is not available.

Acknowledgements

The authors express their gratitude for the support provided by the companies CONCRECON CPC and ESTRUTURAS for the donation, respectively, of concrete and steel profiles used in the push-

out tests of this research. Thanks also go to CAPES (Brazilian Coordination for the Improvement of Higher Education Personnel) and CNPq (National Council for Scientific and Technological Development) for the financial supports for this research. The authors are also thankful to the Structural Laboratory of the University of Brasilia for all tests done along this research.

References

[1] R.P. Johnson, Composite Structures of Steel and Concrete: Beams, Slabs, Columns, and Frames for Buildings, third ed., Oxford, UK, 2004.
[2] S. de Nardin, A. El Debs, State of the art of steel–concrete composite structures in Brazil, in: Proceedings of the Institution of Civil Engineers – Civil Engineering, Civil Engineering Special Issue. ICE Publishing, 2013: pp. 20–27. doi: 10.1680/cien.2013.166.6.20.
[3] H. Galjaard, J.C. Walraven, Behaviour of different types of shear connectors for steel-concrete structures, in: A. Zingoni (Ed.), Structural Engineering, Mechanics and Computation, Elsevier Science Ltd, Cape Town, South Africa, 2001, pp. 385–392, https://doi.org/10.1016/B978-008043948-8/50039-4.
[4] N.M. Hawkins, D. Mitchell, Seismic response of composite shear connections, J. Struct. Eng. 110 (1984) 2120–2136.
[5] EN1994-1-1:2004, Eurocode-4: Design of Composite Steel and Concrete Structures Part 1.1, European Committee for Standardization (CEN), Brussels, Belgium, 2004.
[6] D. Xue, Y. Liu, Z. Yu, J. He, Static behavior of multi-stud shear connectors for steel-concrete composite bridge, J. Constr. Steel Res. 74 (2012) 1–7, https://doi.org/10.1016/j.jcsr.2011.09.017.
[7] H.T. Nguyen, S.E. Kim, Finite element modeling of push-out tests for large stud shear connectors, J. Constr. Steel Res. (2009) 1909–1920, https://doi.org/10.1016/j.jcsr.2009.06.010.
[8] E.Y.L. Chien, J.K. Ritchie, Design and Construction of Composite Floor Systems, 1st Ed, Canadian Inst. of Steel Construction (CISC), Willowdale (Toronto), Ontario, Canada, 1984.
[9] C. Shim, P. Lee, S. Chang, Design of shear connection in composite steel & concrete bridges with precast decks, J. Constr. Steel Res. (2001) 203–219, https://doi.org/10.1016/S0143-974X(00)00018-3.
[10] C.S. Shim, P.G. Lee, T.Y. Yoon, Static behaviour of large stud shear connectors, Eng. Struct. 26 (2004) 1853–1860, https://doi.org/10.1016/j.engstruct.2004.07.011.
[11] R. Hällmark, Prefabricated Composite Bridges - a Study of Dry Deck Joints, Luleå University of Technology, Sweden, 2012.
[12] M.P. Culmo, Prefabricated Composite Bridges in the United States – including total bridge prefabrication, in: Workshop on Composite Bridges with Prefabricated Deck Elements, March 4th 2009, Stockholm, Sweden, 2009.
[13] R. Hällmark, P. Collin, A. Stoltz, Innovative prefabricated composite bridges, Struct. Eng. Int. 19 (2009) 69–78.
[14] M.A. Shahawy, F.D. Hejl, M.T. Kerley, S.R. Kulkarni, M.G. Oliva, M. Lou Ralls, et al., NCHRP (2003) NCHRP Synthesis 324 – Prefabricated Bridge Elements and Systems to Limit Traffic Disruption During Construction, Washington DC, USA, 2003.
[15] AISC, Load and Resistance Factor Design (LRFD) Specification for Structural Steel Building, American Institute of Steel Construction, Chicago, IL, USA, 2010.
[16] O.R. Cavalcante, Study of V-type shear connector for composite steel-concrete beam Ph.D. Dissertation, University of Brasília, Brazil, (In Portuguese), 2010.
[17] M. Titoum, A. Mazoz, A. Benanane, D. Ouinas, Experimental study and finite element modelling of push-out tests on a new shear connector of I-shape, Adv. Steel Constr. 12 (2016) 2016, https://doi.org/10.18057/IJASC.2016.12.4.7.
[18] J.-G. Nie, Y.-X. Li, M.-X. Tao, X. Nie, Uplift-restricted and slip-permitted T-shape connectors, J. Bridge Eng. 20 (2015) 40140731–401407313, https://doi.org/10.1061/(ASCE)BE.1943-5592.0000660.
[19] ABAQUS, User's Manual, Version 6.14-1, Dassault Systèmes Simulia Corp, Providence, RI, USA, 2014.
[20] J. Qureshi, D. Lam, Behaviour of headed shear stud in composite beams with profiled metal decking, Adv. Struct. Eng. 15 (2012) 1547–1558, https://doi.org/10.1260/1369-4332.15.9.1547.
[21] ABAQUS, Theory manual, Version 6.14-1, Dassault Systèmes Simulia Corp, Providence, RI, USA, 2014.
[22] J. Bonilla, L.M. Bezerra, R. Larrúa, C. Recarey, E. Mirambell, Modelación numérica con validación experimental aplicada al estudio del comportamiento de conectores tipo perno de estructuras compuestas de hormigón y acero, Revista Ingeniería de Construcción. 30 (2015) 53–68, https://doi.org/10.4067/S0718-50732015000100005.
[23] X. Xu, Y. Liu, J. He, Study on mechanical behavior of rubber-sleeved studs for steel and concrete composite structures, Constr. Build. Mater. 53 (2014) 533–546, https://doi.org/10.1016/j.conbuildmat.2013.12.011.
[24] J. Lubliner, J. Oliver, S. Oller, E. Oñate, A plastic-damage model for concrete, Int. J. Solids Struct. 25 (1989) 229–326.
[25] J. Lee, G.L. Fenves, Plactic-damage model for cyclic loading of concrete structures, J. Eng. Mech. 124 (1998) 892–900.
[26] S. Oller, J. Oliver, J. Lubliner, E. Oñate, Un Modelo Constitutivo de Daño Plástico para Materiales Friccionales. Parte - 1: Variables Fundamentales, Funciones de Fluencia y Potencial, Revista Internacional de Métodos Numéricos Para Cálculo Y Diseño En Ingeniería. 4 (1988) 397–431.
[27] B. Alfarah, F. López-Almansa, S. Oller, New methodology for calculating damage variables evolution in Plastic Damage Model for RC structures, Eng. Struct. 132 (2017) 70–86.
[28] P. Vermeer, R. De Borst, Non-associated plasticity for soils, concrete and rock, HERON 29 (1984) 3–64.
[29] H. Cornelissen, D. Hordijk, H. Reinhardt, Experimental determination of crack softening characteristics of normal weight and lightweight concrete, Heron. 31 (1986) 45–56.
[30] EN1992-1-1, Eurocode-2: Design of concrete structures. Part 1-1: General rules and rules for buildings, European Committee for Standardization (CEN), Brussels, Belgium, 2004.
[31] E. Ellobody, B. Young, Performance of shear connection in composite beams with profiled steel sheeting, J. Constr. Steel Res. 62 (2006) 682–694.